Journal of the Thai Ceramic Society
Vol.1 [1], pp 1-17 (2025) Research article

Application of Soda-Lime-Silica Cullet as a Fluxing Component in a Vitreous China Ware Casting Body

Danai Arayaphong[1,2], Thanakorn Wasanapiarnpong[1,2,3] *, Uraiwan Leela-adisorn[1], Pattama Jeangkajeng[1], and Sutthima Sriprasertsuk[1]

[1]Department of Materials Science, Faculty of Science, Chulalongkorn University, Bangkok, Thailand
[2]Center of Excellence on Petrochemical and Materials Technology, Chulalongkorn University, Bangkok, Thailand
[3]Upcycled Materials from Industrial and Agricultural Wastes Research Unit, Department of Materials Science, Faculty of Science, Chulalongkorn University, Bangkok, Thailand

*Corresponding author e-mail : thanakorn.w@chula.ac.th

[Received : August 21, 2024 Revised : January 16, 2025 Accepted : January 20, 2025]

Abstract

This study investigates the feasibility of using ground container glass cullet as a partial or complete replacement for feldspar in vitreous sanitary ware casting bodies. Developed bodies, fluxed partially and fully with glass, were evaluated for their casting characteristics and physical properties of fired bodies. The results indicate that slips containing glass powder responded strongly to deflocculants, while most casting properties were satisfactorily maintained. As an auxiliary flux, glass powder increased vitrification in the feldspar-fluxed formula and lowered the maturing temperature. However, excessive glass addition led to a shortened firing range. Complete replacement of feldspar with glass powder was not feasible without increasing the proportion of refractory materials, such as kaolin and flint, in the mixture. This adjustment allows for the inclusion of up to 7.5% glass powder. The reformulated glass-fluxed composition, which retained key characteristics, demonstrated potential as a viable alternative to feldspar-fluxed compositions, exhibiting similar forming and firing behavior. XRD and SEM analyses revealed the presence of various phases and microstructures, particularly cristobalite and mullite, which were associated with certain macrostructural properties.

Keywords: Vitreous China ware casting body, Soda lime silica glass cullet, Fluxing agent, Vitrification

Introduction

Due to rising fuel prices, the trend in the whiteware industry is toward lower firing temperatures. Reducing the maturing temperature of ceramic wares can lead to faster firing cycles, lower fuel consumption, and reduced use of kiln furniture. Studies have shown that firing temperatures can be lowered by substituting various crystalline auxiliary fluxes for feldspar in vitreous floor tiles and semi-vitreous dinnerware bodies[1, 2]. Amorphous glass is another promising fluxing agent that has been successfully applied in clay-based bodies. The potential of using glass powder in porcelain bodies has been explored, with the aim of demonstrating how its fluxing properties can lower required maturing temperatures[3, 4]. In these experiments, glass was introduced as a partial or complete replacement for feldspar and nepheline syenite by weight in typical porcelain stoneware tile batches[5-10]. The body and sample preparation involved a wet process, where the raw materials were ball-milled into slurries, which were then dried, powdered, granulated, and semi-dry pressed into spherical disc specimens.

Slip casting sanitary wares are large vitreous China or porcelain items composed of clay, feldspar, and quartz. Since commercial feldspathic fluxes are among the most expensive raw materials, replacing them with pulverized glass could offer significant economic advantages. There is growing interest among sanitary ware manufacturers in the potential use of recycled glass, with the aim of reducing body costs and lowering firing cone numbers. The principle behind this substitution is that the alkaline earth-alkali content of glass can replace that of feldspar on a total mole fraction basis. However, the higher percentages of CaO and MgO in ground cullet may reduce the viscosity of the feldspathic glassy phase in vitreous bodies, potentially increasing the tendency for pyroplastic deformation in large items under gravity[11]. Besides the mole fraction of fluxing oxides in controlling vitrification, other key properties should be matched or carefully considered to control specific forming and firing characteristics. These critical properties are discussed in the literature[9, 12].

The experiments described in this report were conducted to determine whether glass powder could be used as a partial or complete replacement for feldspar, with the goal of initiating earlier vitrification in normally fired sanitary ware bodies without compromising other fired properties. It was essential to maintain the original controlled slip deflocculation and the casting properties of the modified and reformulated bodies.

Materials and Methods

The raw materials used in this investigation are listed in Table 1, along with their fundamental characteristics. Ball clay is a medium-organic clay sourced from a deposit in Mae Than, Lampang. Kaolin Q composite is a coarse grain, blended and refined clay from a deposit in Ranong. China clay L is a fine grain, washed clay from a deposit in Lampang. The feldspar used was an intermediate spar produced by controlled blending of potassium and sodium feldspars (K, Na) and wet grinding. Flint used was milled-Rayong sand. The glass was ground container glass, specifically colorless soda-lime silica cullet.

The experimental compositions are shown in Table 2. A standard sanitary ware casting body was designated as S. A series of four bodies, labeled G1, G2, G3, and G4, were created where 2%, 4%, 6%, and 8% by weight of glass powder replaced the equivalent amount of feldspar. Body R is a reformulated body in which all feldspar content was replaced by glass powder. Using the whiteware body reformulation method proposed by Phelps[12], body R was calculated by replacing the mole fraction of feldspathic fluxes (0.0340) with the mole fraction of fluxing oxides in glass powder (0.4623). This calculation indicates that a control body fluxed with 26% feldspar would require 7.5% glass. The remaining 18.6% (26 - 7.4 = 18.6%) difference requires an extensive reformulation to ensure that the forming and fired properties of the standard body are maintained. This was achieved by matching "key indicators" such as the SiO_2 to Al_2O_3 ratio, % organic content, % free quartz, % finer than 1 micron, and the methylene blue index to those of the standard body. A comparison of the calculated characteristic data for all bodies is presented in Table 3.

Table 1 Fundamental features of raw materials

Fundamental Features	**Ball Clay**	**Kaolin Q**	**China Clay L**	**Feldspar**	**Flint**	**Glass powder**
Chemical Analysis (%)						
SiO_2	60.40	47.30	63.20	73.84	98.80	71.83
Al_2O_3	25.40	38.40	26.10	14.67	0.59	1.57
Fe_2O_3	1.22	0.82	0.77	0.33	0.05	0.10
TiO_2	0.51	0.05	0.07	0.06	0.07	0.07
CaO	0.30	0.04	0.12	0.51	0.03	10.61
MgO	0.57	0.07	0.27	0.10	0.02	2.47
K_2O	2.40	1.20	5.39	3.60	0.04	0.12
Na_2O	0.32	0.05	0.45	5.01	0.02	13.00
Ignition loss	9.00	12.90	5.16	1.09	0.02	-
Mineral Make Up						
Clays (%)	40.8	86.6	15.6	4.0	1.4	-
Mica (%)	24.0	2.1	51.3	-	-	-
Quartz (%)	30.5	10.7	32.6	28.0	97.9	-
Organic (%)	1.6	0.7	0.5	-	-	-
Feldspathic (%)	-	-	-	66.1	-	-
Mole fraction of fluxing oxides	0.0480	0.0160	0.0720	0.1310	-	0.4520
Particle Size Distribution						
% < 20 μm	99	90	95	83	80	50
% < 10 μm	97	76	78	57	48	24
% < 5 μm	91	54	55	29	24	6
% < 2 μm	72	23	34	8	8	3
% < 1 μm	57	16	25	2	3	1
% < 0.5 μm	40	10	16	-	-	-
% < 0.2 μm	21	4	8	-	-	-
Methylene Blue Index (meq/100g)	7.5	2.4	3.4	-	-	-

Table 2 Experimental body compositions

Materials (%)	**Body S**	**Body G1**	**Body G2**	**Body G3**	**Body G4**	**Body R**
Ball Clay	35	35	35	35	35	32
Kaolin Q	12	12	12	12	12	18
China Clay L	13	13	13	13	13	20
Feldspar	26	24	22	20	18	-
Flint	14	14	14	14	14	22.5
Glass powder	-	2	4	6	8	7.5

Table 3 Fundamental features of experimental bodies

Fundamental Features	Body S	Body G1	Body G2	Body G3	Body G4	Body R
Chemical Analysis (%)						
SiO_2	68.10	68.02	67.98	67.94	67.90	68.10
Al_2O_3	20.68	20.51	20.25	19.99	19.73	20.54
Fe_2O_3	0.71	0.55	0.55	0.57	0.57	0.70
TiO_2	0.23	0.21	0.21	0.21	0.21	0.23
CaO	0.26	0.46	0.67	0.87	1.00	0.93
MgO	0.25	0.30	0.34	0.39	0.44	0.32
K_2O	2.63	2.56	2.49	2.42	2.35	2.09
Na_2O	1.47	1.64	1.80	1.96	2.12	1.18
Ignition loss	5.70	5.67	5.64	5.62	5.60	5.38
Mineral Make Up						
Clays (%)	27.9	27.9	27.8	27.7	27.6	32.6
Mica (%)	15.4	15.4	15.4	15.4	15.4	18.4
Quartz (%)	37.2	36.7	36.1	35.5	34.9	40.2
Organic (%)	0.7	0.7	0.7	0.7	0.7	0.7
Feldspathic (%)	17.2	15.9	14.5	13.2	11.9	-
Mole fraction of fluxing oxides	0.0617	0.0681	0.0742	0.0804	0.0861	0.0624
Particle Size Distribution						
% < 20 μm	91	90	89	88	88	89
% < 10 μm	75	75	73	73	72	73
% < 5 μm	57	56	56	55	54	55
% < 2 μm	35	35	35	35	34	36
% < 1 μm	26	26	26	25	25	26
% < 0.5 μm	17	17	17	17	17	18
% < 0.2 μm	9	9	9	9	9	9
Methylene Blue Index (meq/100g)	3.36	3.36	3.36	3.36	3.36	3.50

The raw materials were processed into powdered form to ensure uniform mixing and dispersion. Ball clay and China clay were ground manually using a mortar and pestle, then sieved to pass through a 20-mesh screen. Feldspar and flint, supplied as 325-mesh milled non-plastic powders, were used without further modification. The cullet was crushed and subsequently wet ball-milled in a porcelain jar mill with porcelain grinding media for six hours to achieve a particle size finer than 170-mesh. Test slips were prepared using the direct method, formulated as 70% solids by weight in partially deflocculated slurries and mixed with a variable-speed mixer to ensure homogeneity.

A 3,000-gram batch (on a dry body basis) batch was prepared for each body using the following procedure: dark ball clay was blunged at high speed with a pre-calculated amount of distilled water, to which 0.02% sodium carbonate (dry body basis) had been added. As the ball clay thickened, sodium silicate was introduced to ensure good fluidity and turbulence. Blunging continued for 15 minutes, and the ball clay slurry was then passed through a 100-mesh screen. Kaolin Q and China clay L were subsequently added with adjusted sodium silicate, and each was blunged for 15 minutes. Feldspar, glass powder, and flint were then introduced in that order, with additional sodium silicate as needed to maintain a sluggish flow, indicating under-deflocculation.

The finished slips were blunged for an additional half hour and aged for 24 hours in closed containers. The total preparation time per batch was 2 hours. The aged slips were adjusted to a specific gravity of 1.76 and progressively deflocculated to achieve near-minimum viscosity. After each addition of deflocculant, viscosity was measured with a Brookfield RVT viscometer using a No. 3 spindle at 20 rpm. These values were plotted against % sodium silicate to draw a deflocculation curve. Near-fully deflocculated slips (just short of maximum fluidity) were cast in conditioned plaster cup molds for 16 minutes, then drained at an angle for 10 minutes. The cast cups were inspected for drainage quality, feel, mold release, and wall thickness, and the rate of casting was recorded. Moist cups were weighed, dried at 105°C for 24 hours, and cooled in desiccators. Moisture loss was reported as the percentage of retained water based on dry weight.

Test pieces were cast into three forms: round bars with a diameter of 1.5 cm and a length of 15 cm; rectangular bars measuring 17.5 cm by 2.3 cm by 0.5 cm; and smaller rectangular samples measuring 3.1 cm by 0.8 cm by 0.4 cm. These samples were fired in an electric kiln at temperatures of 1140°C, 1170°C, 1200°C, and 1230°C, with a heating rate of 150°C per hour and a 30-minute soak at the peak temperature.

Fired cylindrical bars were measured for linear firing shrinkage[13] and modulus of rupture[14], and were also tested for water absorption and bulk density[15]. Rectangular sag test green bars were fired on refractory supports, as shown in Fig. 1. (A). Pyroplastic deformation or warpage was measured and reported in millimeters, as shown in Fig. 1. (B).

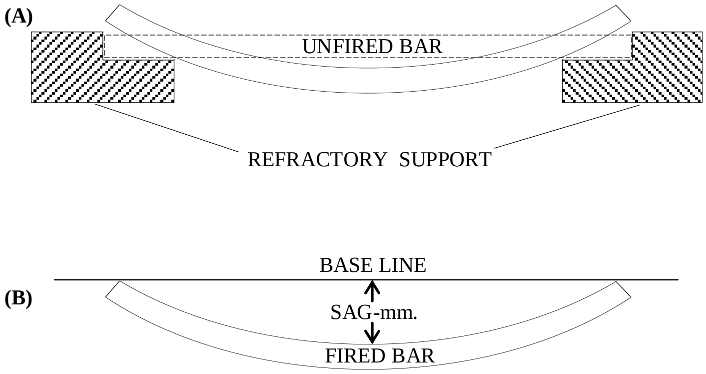

Fig. 1. Diagram of the sagging bar test set up (A) unfired bar, (B) fired bar.

Small rectangular samples were used to measure linear reversible thermal expansion using a NETZSCH DIL402 dilatometer, with measurements taken from 30 °C to 700 °C. Phase compositions were determined using an X-ray diffractometer (BRUKER AXS Advanced D8) operating in step scan mode with a step size of 0.02°, and a scan time of 1.2 seconds per step. Powdered samples were analyzed using Cu-K$_\alpha$ radiation with a 2-theta range of 5-70°.

The microstructure was observed using a scanning electron microscope (JEOL JSM 5800 LV). Each vitrified test bar was cross-sectioned, then wet-ground with silicon carbide papers (120, 240, 600, 1200) and polished with a 1 µm diamond solution. The samples were then acid-etched with a 10% HF solution for 20 seconds, and finally, the etched surfaces were sputter-coated with gold.

Results and discussion

The deflocculation behaviors of the experimental slips are shown in Fig. 2. All slip batches with a specific gravity of 1.76 achieved a minimum viscosity ranging from 600 to 450 centipoises (cps) (mPa·s). The amount of sodium silicate required for adjustment varied among different body slips. The deflocculation response and viscosity data for the standard slip of body S and the glass-fluxed body slips indicate that replacing feldspar with 2% to 8% glass powder resulted in a sharper response to sodium silicate and increased fluidity in the modified slips. As the percentage of glass increased, the amount of deflocculant needed to initiate flow and achieve maximum fluidity decreased.

This change in rheological behavior may be partly due to the interaction of glass powder with the organic content in the ball clay. The continued reaction of hydrolyzed sodium leached from the glass progressively deflocculated the organic-containing casting bodies[16]. At higher glass content (~8%), the interaction of sodium from both soda ash and glass with organic matter after aging also led to staining of casts and molds. This was observed on the surface beneath the cast after pouring the aged, fully deflocculated slips onto clean plaster molds.

Differences in particle size distribution between glass powder and feldspar, which led to small changes in the intermediate size range, also affected the flow behavior of these slips[17]. Increased slip fluidity allows for the introduction of calcium salts and/or the use of higher specific gravity to improve casting performance[16]. When China clay and flint were increased and ball clay was reduced in the reformulated body R, the viscosity and deflocculation response were brought closer to those of the control slip batch.

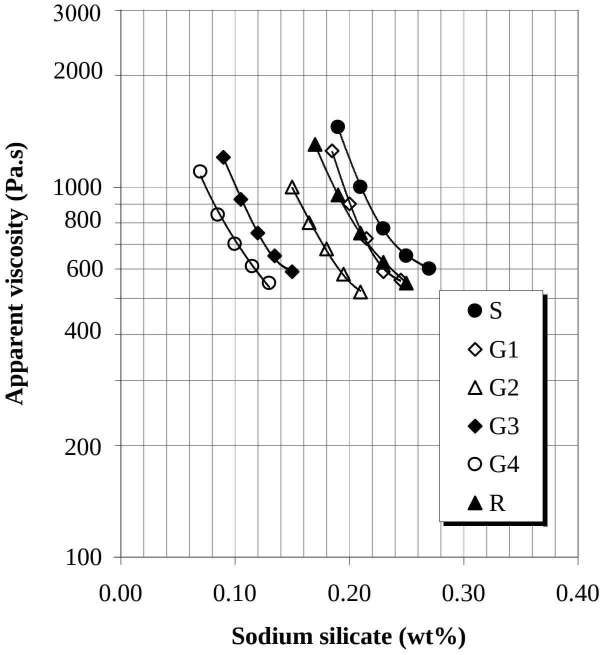

Fig. 2. Deflocculation curves for experimental casting bodies.

Table 4 summarizes the casting properties of the slips corresponding to all body batches, showing that they exhibited good draining properties, being quick and clean. After draining, the shiny surfaces of the casts became dull, and the skin was stripped from the mold and handled with fingers. The feel of the casts was satisfactory, demonstrating adequate plasticity. All casts could be released easily after setting in the mold for 10 minutes. Body S displayed a cast thickness of 6.8 mm after 16 minutes of casting.

Despite their greater fluidity, replacing feldspar with coarser glass powder increased the casting rate, as the percentage of particles finer than 1 micron decreased while methylene blue indices remained constant. The cast cups exhibited higher water retention, ranging from 19.1% to 21.4%, as the amount of glass increased.

A quick mold release with high water retention in body R may present challenges, as the high clay content results in prolonged drying times for the casts. Additionally, the piece cannot be left in the mold for extended periods for working and trimming, which increases the risk of cracking in larger items.

To examine the interrelation of the investigated bodies, the data obtained for the physical fired properties are plotted in Fig. 3. to 7. In general, linear firing shrinkage, bulk density, sagging, and modulus of rupture increased with firing temperature, while water absorption decreased. The control body S, containing feldspar, exhibited lower linear firing shrinkage compared to the glass-fluxed bodies (G1 to G4) at all firing temperatures. Shrinkage in body S increased more rapidly from 1140 °C to 1200 °C, reaching a maximum at 1230 °C. In contrast, shrinkage values for bodies G1 to G4 were similar at 1140 °C. At each firing temperature from 1170 °C to 1230 °C, shrinkage for G1, G2, and G3 increased with the progressive incorporation of glass powder. Body G1 reached maximum shrinkage at 1230 °C, while bodies G2 and G3 showed relatively constant shrinkage from 1200 °C to 1230 °C. There were no signs of blistering or overfiring in G2, but body G3 exhibited slight overfiring at 1230 °C. Body G4 shrank more rapidly than the others, with a significant decrease in shrinkage beyond 1200 °C due to gas expansion trapped in the glassy melt, indicating overfiring[18].

The reformulated body R had a shrinkage rate similar to the control body. Water absorption trends were consistent with shrinkage data. The structure of the feldspar-fluxed body was more open, whereas increased glass powder content reduced open porosity. Vitrification was fully established at 1230 °C for bodies S and G1. Higher glass content led to earlier vitrification and lower maturing temperatures. Bodies G2, G3, and G4 vitrified at 1200 °C, with G3 and especially G4 approaching vitrification at 1170 °C. At 1230 °C, body G4 showed signs of a glassy appearance, indicating overfiring. The reformulated body R matured at 1230 °C but not as pronouncedly as the standard body.

A comparison of fundamental data in Table 1 shows that glass has a coarser particle size distribution than feldspar, as determined by a laser particle size analyzer (Master Sizer 2000, Malvern). Finer-glass powder would act as a more effective auxiliary flux[19]. Bulk density followed a similar trend, with slight increases at 1140 °C and 1170 °C across all samples. Bodies S and G1 showed a substantial increase in bulk density, reaching a maximum at 1230 °C. Bodies G2, G3, and G4 reached maximum density at 1200 °C, with G2 remaining unchanged but decreasing for G3 and G4 at 1230 °C. Bloating occurred in fired specimens G3, reducing bulk density beyond the point of dense sintering. Overfiring was more pronounced in G4, which contained the highest amount of glass. The bulk density changes in the reformulated body were similar to body S but at a slower rate.

The relationship between fired modulus of rupture (MOR) and firing temperatures showed a gradual increase in strength up to the vitrification point. The strength curve for overfired samples G3 and G4 flattened from 1200 °C to 1230 °C. Body R exhibited lower fired MOR compared to body S at each firing temperature. It can be concluded that glass powder is not as effective or powerful as feldspar in providing the same amount of fluxing oxides.

Pyroplastic deformation increased with higher firing temperatures in all cases and also increased with the amount of glass as temperatures approached vitrification. Glass powder contains significant amounts of CaO and MgO, which react vigorously with feldspar, making the feldspathic glassy phase more fluid and increasing its tendency to deform under gravity during firing. The most pronounced pyroplastic sag occurred in body G4, which had the highest glass content, when the temperature was high enough to cause overfiring.

However, the pre-reacted flux (glass) did not cause excessive slumping or warping in the reformulated body. Sag bar tests for glass-fluxed body R and feldspar-fluxed body S demonstrated nearly identical behavior, although the degree of vitrification in the reformulated batch was lower.

It is evident that, considering the effect of heat on the constituents of clay-glass-flint bodies, the glass melt, like feldspar, dissolves the clay and silica. This results in higher alumina and silica content, which increases the viscosity of the glass and helps to prevent distortion[20].

The linear thermal expansion curves are shown in Fig. 8. Table 5 displays the coefficient of thermal expansion in the temperature range of 100-500 °C and the percentage expansion at 600 °C. The thermal expansion of the vitrified standard body sample is 0.45% at 600 °C. Glazes applied to once-fired sanitary ware mature at 1200 °C to 1220 °C and have yield point values approximately at 600 °C, which is why the percent expansion is quoted at this temperature[21].

The reversible thermal expansion coefficient increased gradually with the incorporation of pulverized glass powder. The increase in glass content did not lead to a significant dissolution of crystalline silica, as indicated by XRD, since the characteristic inflection point at 573 °C for quartz transformation and the total expansion remained unchanged. The addition of glass containing appreciable amounts of MgO initiated an inflection in the thermal expansion curves between 150 °C and 220 °C, indicating the presence of cristobalite. The most distinct cristobalite inversion was observed in body G4, which contained 8% glass, with expansion increasing to 0.49% at 600 °C.

The conversion of quartz to cristobalite occurs more rapidly in low-viscosity glass when the rate of transformation exceeds the rate of quartz dissolution[22]. A small amount of cristobalite in whiteware bodies helps prevent glaze crazing due to the inversion from high to low-temperature forms of cristobalite during cooling. This provides an advantage for glaze-body fit, as the inversion is accompanied by contraction, which puts the glaze into compression[21]. However, the cristobalite content should be carefully controlled, and precautions should be taken to prevent dunting during cooling, particularly in the critical temperature range around 220 °C. The percentage expansion at 600 °C for the reformulated glass-fluxed body is quite close to that of the standard body at the same maturing temperature.

The X-ray diffraction pattern (Fig. 9.) of various fired body specimens revealed that the standard body composition fired at 1230 °C contains major crystalline phases, namely quartz, mullite, and a small amount of cristobalite. Replacing feldspar with pulverized glass enhanced the formation of cristobalite, indicated by a peak at 4.07 Å. The cristobalite content increased with the progressive substitution of glass for feldspar. Among the glass-containing bodies, body G4 exhibited the highest cristobalite development, despite vitrifying at 1200 °C. The quantity of residual quartz in the fired mass remained unchanged, but the mullite content appeared lower in bodies G3 and G4, as evidenced by their peak intensity. The reformulated body fired at 1230 °C showed crystalline phases similar in intensity to those found in the control batch.

The microstructure study of vitrified samples using SEM revealed the presence of unreacted free quartz grains with a surrounding solution rim, as shown in the micrograph in Fig. 10. Notably, a large quartz grain in the right-hand corner exhibits a deep solution rim and has developed a crack in its interior due to thermal stress between the large grain and the surrounding glass phase. Smaller quartz grains, however, show no signs of fissures. The clay and flux react to form an alkali alumino-silicate glass, which binds the original quartz particles together. This crystalline component acts as a refractory skeleton, preventing the vitreous structures of vitreous China bodies from collapsing into the glass matrix during vitrification[23].

Fig. 11. illustrates scaly and cuboidal shapes associated with distinct stubby primary mullite forming an interlaced mat in the kaolin relicts. The observed crystal sizes are <0.5 μm, with elongated prismatic crystals ranging from 1-1.5 μm in length and 0.2-0.4 μm in width. Similar descriptions of the elongated needle-shaped primary mullite phase were reported by Comer[24] and Grum-Grzhimailo[25], who described them as tabular and elongated crystals with a preferred orientation arranged parallel to one another. An appreciable amount of smaller, more elongated secondary mullite needles crystallized from the feldspar-silica melt (Fig. 10.). The higher aspect ratio of secondary mullite, with its thinner needle-like crystals interlocking and distributing throughout the vitreous body, contributes to greater fired strength compared to primary mullite[26].

Replacing feldspar with glass powder is believed to enhance the reaction between quartz, clay, and the feldspathic melt, producing a more liquid phase and thereby increasing pyroplastic deformation. In the reformulated glass-fluxed body without feldspar, the glass melts and eventually forms crystals of mullite and a partial solution of clay and finer silica grains, making the melt more viscous. Differences in the viscosity and chemical composition of the molten glassy phase can suppress or enhance the crystallization of secondary mullite[27]. However, the shorter firing range of soda-lime glass-containing bodies makes them well-suited for fast firing processes. Additionally, their adaptability allows for the design of lightweight ceramic products, further enhancing their suitability for fast firing applications.

Fig. 12. shows micrographs of vitrified bodies (1230 °C) for S, G1, G2, and R, respectively. There is a better development of interlocked secondary mullite in the feldspar relicts compared to the less dense mullite structure in bodies G3 and G4, which were vitrified at a lower temperature (1200 °C). The Al_2O_3 content is slightly lower in bodies G3 and G4 since the glass composition contains 1.57% Al_2O_3, much less than the 14.67% found in feldspar. Because Al_2O_3 has low mobility in the glassy phase, alkali ions from feldspar migrate across the boundary into the dehydroxylated clay relicts. In the alkali-depleted feldspar relicts, the lower Al_2O_3 content results in sparser secondary mullite in the melt [22].

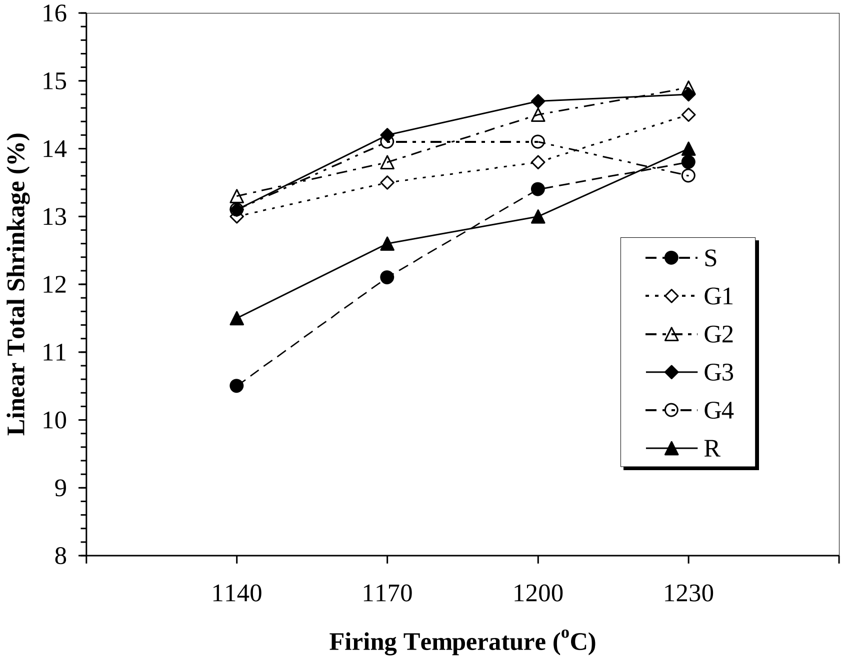

Fig. 3. Effect of firing temperature on firing shrinkage.

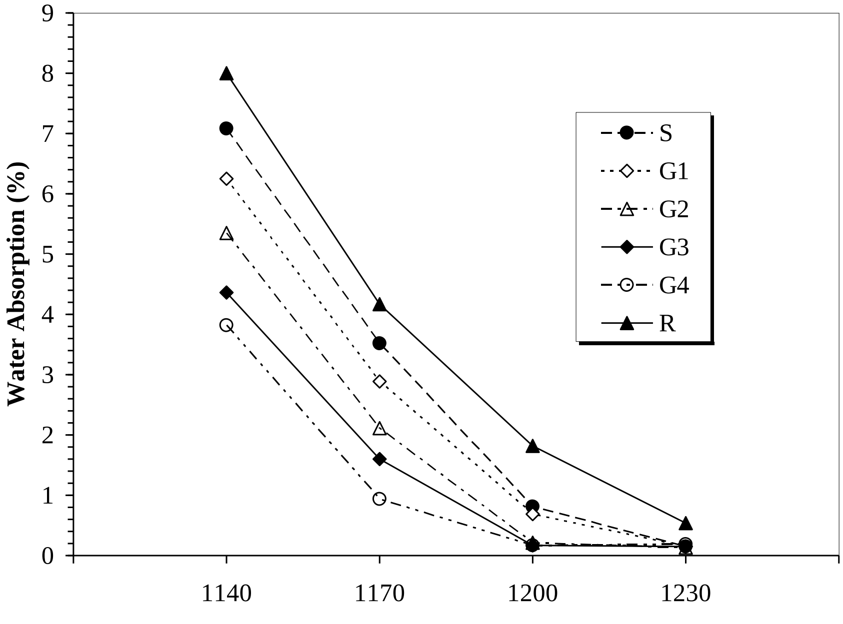

Fig. 4. Effect of firing temperature on water absorption.

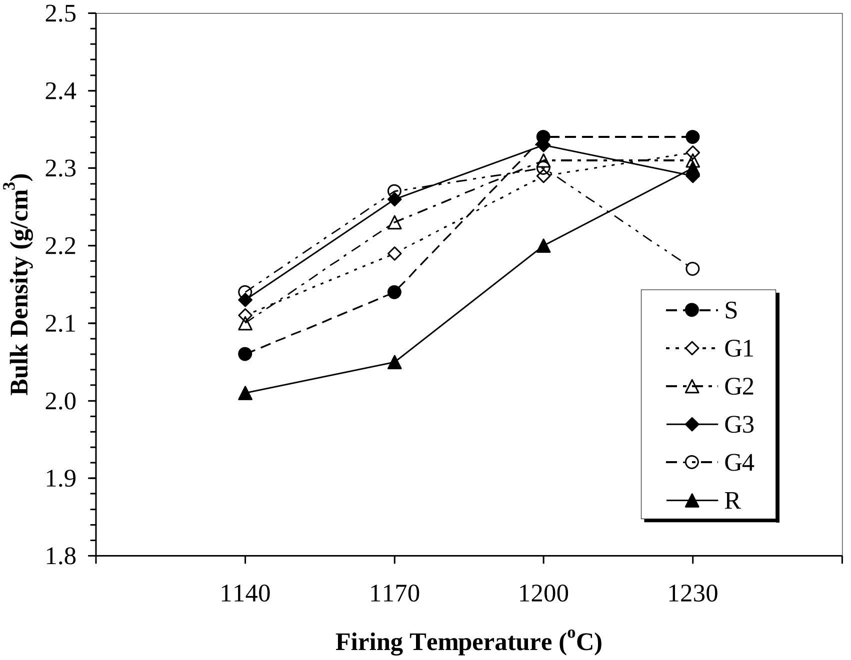

Fig. 5. Effect of firing temperature of fired bulk density.

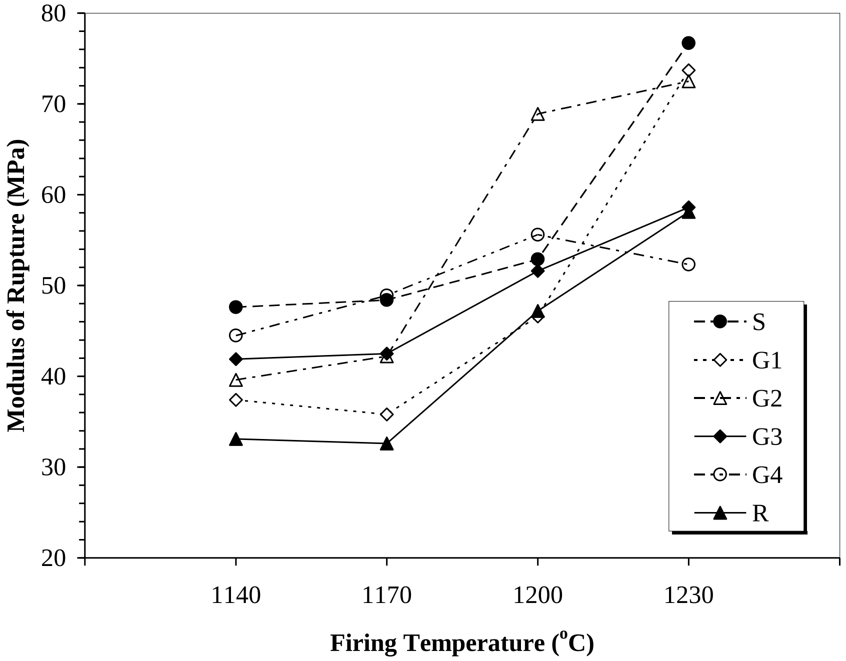

Fig. 6. Effect of firing temperature on fired modulus of rupture

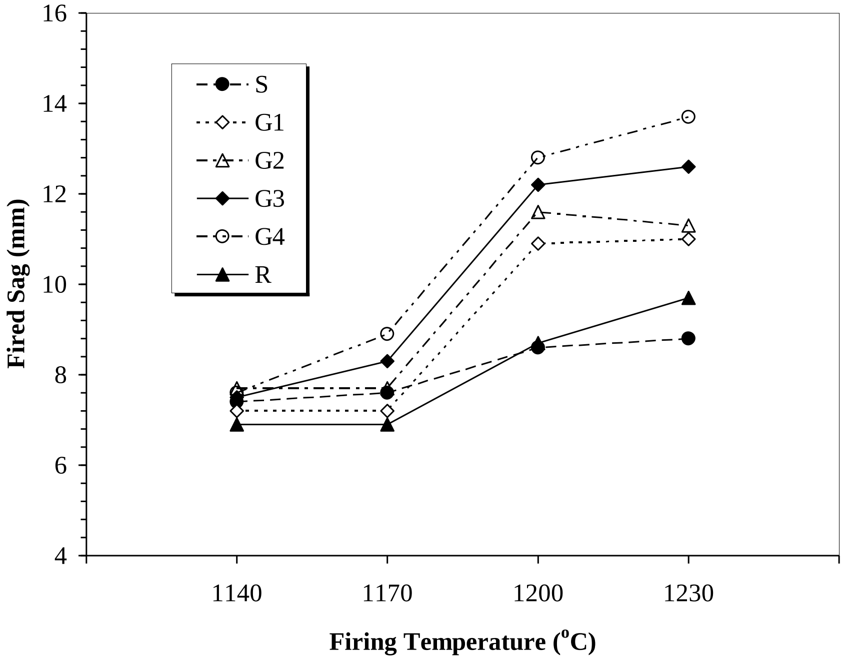

Fig. 7. Effect of firing temperature on pyroplastic deformation.

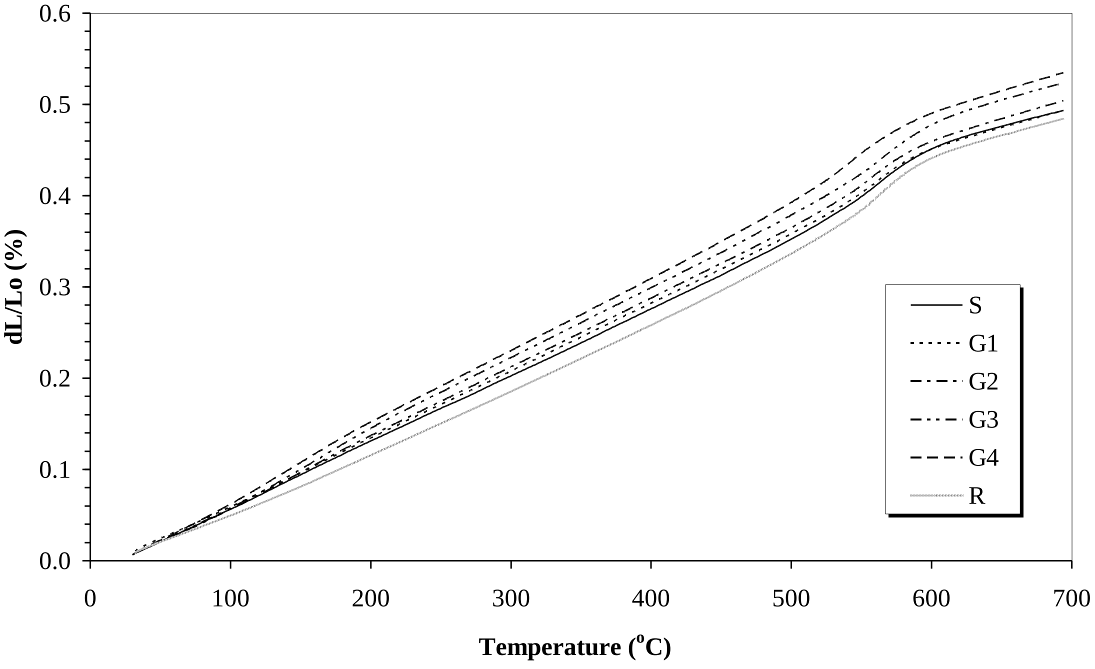

Fig. 8. Linear reversible thermal expansion of the experimental bodies.

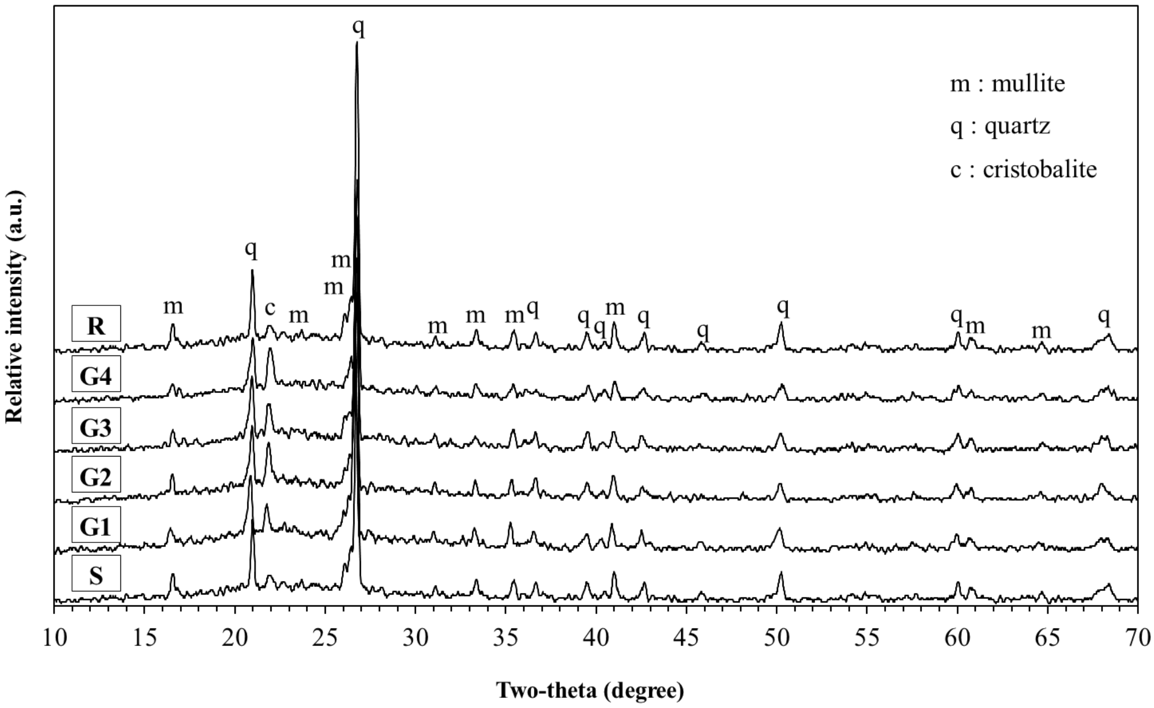

Fig. 9. XRD patterns of the experimental bodies.

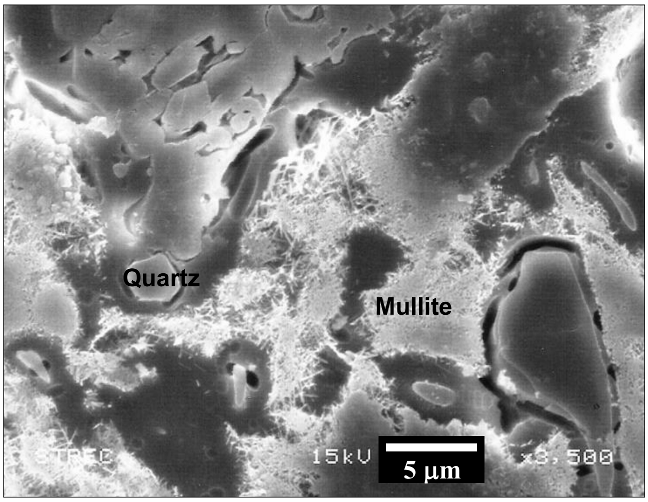

Fig. 10. SEM micrograph of vitrified at 1230 °C of sample R with solution rim around quartz grain.

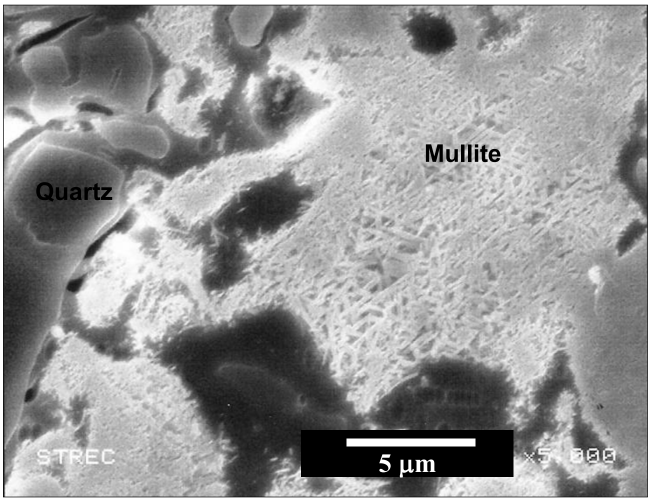

Fig. 11. SEM micrograph of vitrified at 1230 °C of sample R with small and shorter cuboidal primary mullite crystals.

Table 4 Casting properties

Body designation	**Casting rate (mm/16min)**	**Drain quality**	**Feel quality**	**Mold release**	**Retained water (%)**	**Staining**
S	6.80	Clean	Good	Good	19.10	None
G1	7.00	Clean	Good	Good	18.94	None
G2	7.00	Clean	Good	Good	19.99	None
G3	6.90	Clean	Good	Good	19.69	None
G4	7.10	Clean	Good	Good	19.50	Slightly
R	7.35	Clean	Good	Good	21.35	Slightly

Table 5 Linear thermal expansion coefficient at 100-500 °C and expansion at 600 °C of the test bodies.

Body designation (Firing temp.)	**$\alpha \times 10^{-6}$ °C^{-1} (100-500 °C)**	**Expansion at 600 °C (%)**
S (1230 °C)	7.4017	0.45
G1 (1230 °C)	7.4716	0.45
G2 (1200 °C)	7.7214	0.46
G3 (1200 °C)	8.0258	0.48
G4 (1200 °C)	8.2683	0.49
R (1230 °C)	7.1758	0.44

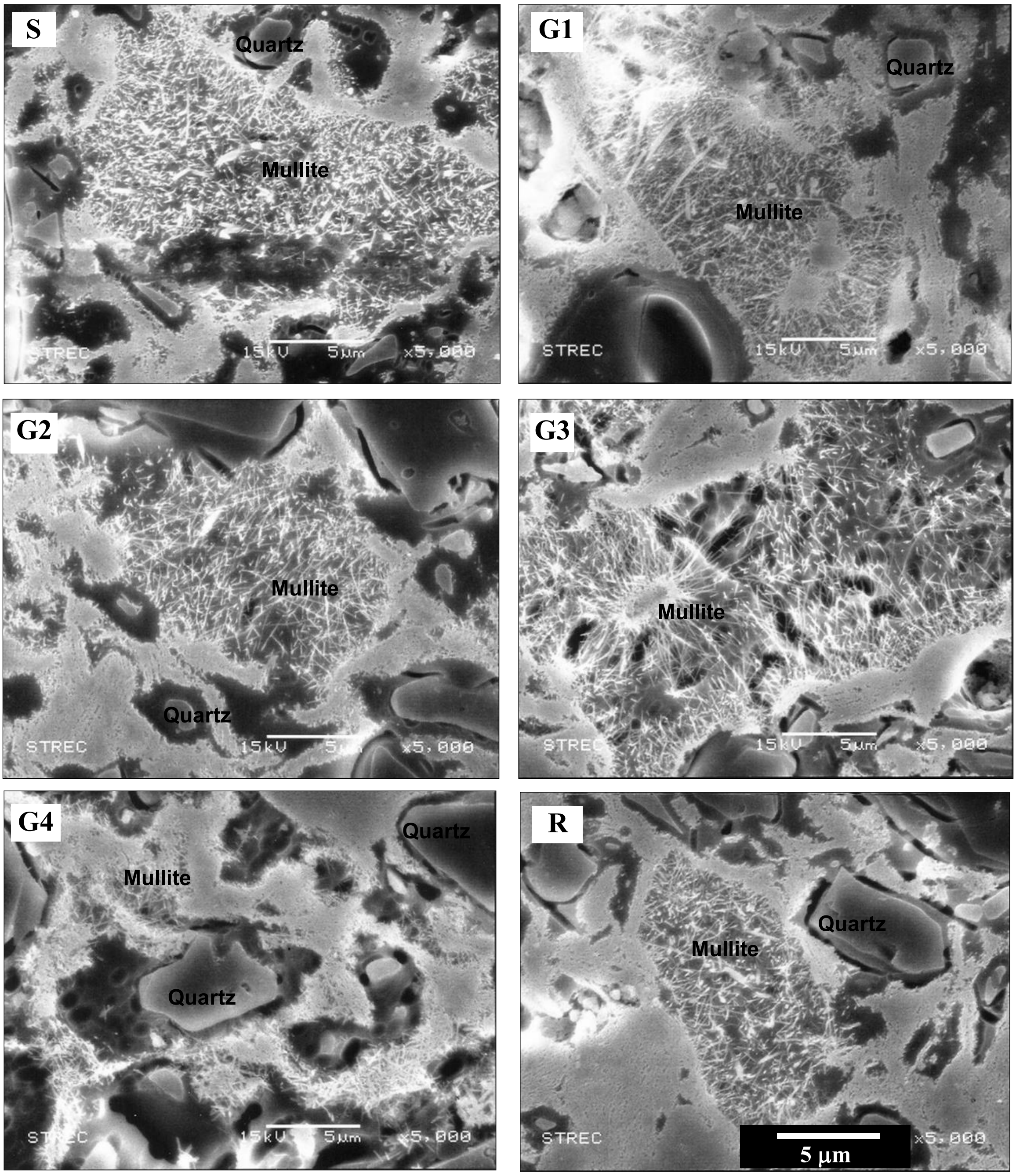

Fig. 12. SEM micrographs of vitrified at 1230 °C of sample S, G1, G2, G3, G4, and R.

Conclusion

It is feasible to replace feldspathic fluxes in vitreous sanitary ware casting bodies with ground container glass cullet. The glass-containing slips exhibited a significant deflocculating effect on the organic matter in ball clay, resulting in steeper deflocculation curves compared to the control slip batch. By employing the proposed reformulation method, which adjusts key indicators to match target values from the control body, the rheological behavior of the modified slips closely resembled that of the control slip. Most casting properties of the modified bodies were satisfactorily maintained with glass powder levels of less than 6%. At higher glass percentages, casting behavior deteriorated slightly.

Partial replacement of feldspar with glass powder accelerated densification, increased vitrification, and reduced the maturing temperature by 30 °C (equivalent to two pyrometric cones). However, this substitution resulted in lower bulk density and fired strength. Complete replacement of feldspar with glass in the reformulated body achieved firing characteristics reasonably close to those of the control body. The increase in thermal expansion of glass-containing bodies is attributed to a higher cristobalite content. The lower fired modulus of rupture (MOR) and greater pyroplastic deformation observed in glass-fluxed bodies may be partly due to fewer and less tightly interlocked secondary mullite crystals in their structures.

References

[1] Morse, G. T. (1948). Use of dolomite as an auxiliary flux in floor tile. Journal of the American Ceramic Society, 31(3), 67-70.

[2] Kyonka, I. C., Cook, R. L. (1953). The effect of fluxes on the properties of semi-vitreous dinnerware. American Ceramic Society Bulletin, 32(7), 233-238.

[3] Zimmer, A., Bragança, S. R. (2019). A review of waste glass as a raw material for whitewares. Journal of Environmental Management, 244, 161-171.

[4] Marinoni, N., D'Alessio, D., Diella, V., Pavese, A., Francescon, F. (2013). Effects of soda–lime–silica waste glass on mullite formation kinetics and micro-structures development in vitreous ceramics. Journal of Environmental Management, 124, 100-107.

[5] Matteucci, F., Dondi, M., Guarini, G. (2002). Effect of soda-lime glass on sintering and technological properties of porcelain stoneware tiles. Ceramics International, 28(8), 873-880.

[6] Tucci, A., Esposito, L., Rastelli, E., Palmonari, C., Rambaldi, E. (2004). Use of soda-lime scrap-glass as a fluxing agent in a porcelain stoneware tile mix. Journal of the European Ceramic Society, 24(1), 83-92.

[7] Tarvornpanich, T., Souza, G. P., Lee, W. E. (2005). Microstructural Evolution on Firing Soda–Lime–Silica Glass Fluxed Whitewares. Journal of the American Ceramic Society, 88(5), 1302-1308.

[8] Njindam, O. R., Njoya, D., Mache, J. R., Mouafon, M., et al. (2018). Effect of glass powder on the technological properties and microstructure of clay mixture for porcelain stoneware tiles manufacture. Construction and Building Materials, 170, 512-519.

[9] Bragança, S. R., Bergmann, C. P. (2009). Porcelain Casting Slips Formulated with Waste Glass. International Journal of Applied Ceramic Technology, 6(2), 264-269.

[10] Baccarin, L. I. P., Bielefeldt, W. V., Bragança, S. R. (2023). Prediction of glass phase viscosity in firing traditional ceramics and porcelain tiles with waste glass powder. Open Ceramics, 15, 100417.

[11] Holridge, D. A., Edwards, H. (1964). Vitrification in some non porous pottery bodies. Transactions of the British Ceramic Society, 63(6), 261-287.

[12] Phelps, G. W. (1976). Reformulation of whiteware bodies. American Ceramic Society Bulletin, 55(5), 528-532.

[13] ASTM C326-09 (2014) Standard Test Method for Drying and Firing Shrinkages of Ceramic Whiteware Clays.

[14] ASTM C674-13 Standard Test Methods for Flexural Properties of Ceramic Whiteware Materials.

[15] ASTM C373-16 Standard Test Method for Water Absorption, Bulk Density, Apparent Porosity, and Apparent Specific Gravity of Fired Whiteware Products.

[16] Phelps, G. W. (1959). The role of organic matter in slip casting. American Ceramic Society Bulletin, 38(5), 246-250.

[17] Phelps, G. W., McLaren, M. G. (1978). Particle Size Distribution and Slip Properties. John Wiley & Sons, New York.

[18] Lawrence, W. G., West, R. R. (1982). Ceramic Science for the Potter. Chilton Book Company, New York.

[19] Tyrrell, M. E., Goode, A. H. (1972). Waste Glass as a Flux for Brick Clays. Report of Investigation 7701, U. S. Dept. of Interior, Bureau of Mines, Washington.

[20] Norton, F. H. (1970). Fine Ceramics. John Wiley, New York.

[21] Ryan, W., Radfad, C. (1987). Whitewares: Production, Testing and Quality Control. Pergaman Press, Oxford.

[22] Lundin, S. T. (1959). Studies on Triaxial Whiteware Bodies. Almqvist & Wiksell, Stockholm.

[23] Dinsdale, A., Wilkinson, W. T. (1966). Strength of Whiteware Bodies. Proceedings of the British Ceramic Society, 6, 119-136.

[24] Comer, J. J. (1960). Electron Microscopy Studies of Mullite Development in Fired Kaolinites. Journal of the American Ceramic Society, 43(7), 378-384.

[25] Grum-Grzhimailo, O. S. (1971). Primary Mullite in Low-Temperature Porcelain. Glass and Ceramic, 28(5), 313-315.

[26] Carty, W. H., Senapati, U. (1998). Porcelain - Raw Materials, Processing, Phase Evolution, and Mechanical Behavior. Journal of the American Ceramic Society, 81(1), 3-20.

[27] Braganca, S. R., Bergmann, C. P. (2004). Traditional and glass powder porcelain: Technical and microstructure analysis. Journal of the European Ceramic Society, 24(8), 2383-2388.